Array Processing for Nonstationary Interference Suppression in DS/SS Communications Using Subspace Projection Techniques

Yimin Zhang, *Senior Member, IEEE,* and Moeness G. Amin, *Fellow, IEEE*

Abstract—**Combined spatial and time–frequency signatures of signal arrivals at a multisensor array are used for nonstationary interference suppression in direct-sequence spread-spectrum (DS/SS) communications. With random PN spreading code and deterministic nonstationary interferers, the use of antenna arrays offers increased DS/SS signal dimensionality relative to the interferers. Interference mitigation through a spatio-temporal subspace projection technique leads to reduced DS/SS signal distortion and improved performance over the case of a single antenna receiver. The angular separation between the interference and desired signals is shown to play a fundamental role in trading off the contribution of the spatial and time–frequency signatures to the interference mitigation process. The expressions of the receiver signal-to-interference-noise ratio (SINR) implementing subspace projections are derived, and numerical results are provided.**

Index Terms—**Array processing, direct-sequence spread-spectrum communication, interference suppression, subspace projection, time–frequency distribution.**

I. INTRODUCTION

THERE are several methods that have been proposed for interference suppression in direct-sequence spread-spectrum (DS/SS) communications. Most have been related to one domain of operation [1], [2]. These methods include the narrowband interference waveform estimation [3], [4], frequency domain interference excision [5], zero-forcing techniques [6], adaptive subspace-based techniques [7], [8], and minimum-mean-square error (MMSE) interference mitigation techniques [9].

Nonstationary interferers, which have model parameters that change with time, are particularly troublesome due to the inability of a single domain mitigation algorithm to adequately remove their effects. The recent development of the quadratic time–frequency distributions (TFDs) for improved signal power localization in the time–frequency plane has motivated several new approaches for excision of interference with rapidly time-varying frequency characteristics in the DS/SS communication systems. Comprehensive summary of TFD-based interference

excision is given in [10]. The two basic methods for time–frequency excision are based on notch filtering and subspace projections. Utilization of the interference instantaneous frequency (IF), as obtained via TFDs, to design an open-loop adaptive notch filter in the temporal domain, has been thoroughly discussed in [11] and [12]. Subspace projection methods, which are commonly used for mitigating narrowband interference [13], [14], have been recently introduced for suppression of frequency modulated (FM) interference and shown to properly handle multicomponent interference, reduce the self-noise, and improve the receiver performance beyond that offered by other time–frequency based techniques [15]–[17].

The main purpose of this paper is to integrate spatial and temporal processing for suppression of nonstationary interferers in DS/SS communication systems. Specifically, we extend the projection-based interference mitigation techniques in [15]–[17] to multisensor array receivers. The proposed multisensor interference excision technique builds on the offerings of quadratic time-frequency distributions for estimation of 1) the time–frequency subspace and time–frequency signature of nonstationary signals and 2) the spatial signature of nonstationary sources using direction finding and blind source separations. With the knowledge of the time–frequency and spatial signatures, the objective is to effectively suppress strong nonstationary interferers with few array sensors. The proposed technique does not require the knowledge of the array response or channel estimation of the DS/SS signal, but it utilizes the distinction in both of its spatial- and time–frequency signatures from those of the interferers that impinge on the array. With the combined spatial-time–frequency signatures, the projection of the data vector onto the subspace orthogonal to that of the interferers leads to improved receiver performance over that obtained using the subspace projection in the single-sensor case.

The rest of the paper is organized as follows. In Section II, the signal model is described. Section III briefly reviews the subspace projection technique. We present in Section IV blind beamforming based on subspace projection and derive the receiver output signal-to-interference-plus-noise ratio (SINR). Several numerical results are given in Section V. Section VI concludes this paper.

II. SIGNAL MODEL

In DS/SS communications, each symbol is spread into $L = T/T_c$ chips, where T and T_c are, respectively, the symbol duration and chip duration. We use discrete-time form, where all

The authors are with the Department of Electrical and Computer Engineering, Villanova University, Villanova, PA 19085 USA (e-mail: yimin@ieee.org; moeness@ece.villanova.edu).

signal arrivals are sampled at the chip-rate of the DS/SS signal. The symbol-rate source signal is denoted as $s(n)$, and the aperiodic binary spreading sequence of the nth symbol period is represented by $c(n, l) \in \pm 1, l = 0, 1, \ldots, L - 1$. The chip-rate sequence of the DS/SS signal can be expressed as

$$d(k) = s(n)c(n, l) \quad \text{with } k = nL + l. \tag{1}$$

For notational simplicity, we use $c(l)$ instead of $c(n, l)$ for the spreading sequence.

We consider an antenna array of N sensors. The propagation delay between antenna elements is assumed to be small relative to the inverse of the transmission bandwidth so that the received signal at the N sensors are identical to within complex constants. The received signal vector of the DS/SS signal at the array is expressed by the product of the chip-rate sequence $d(k)$ and its spatial signature $\underline{h}$

$$\underline{x}_s(k) = d(k)\underline{h}. \tag{2}$$

The channel is restricted to flat fading and is assumed fixed over the symbol length, and as such, $\underline{h}$ in the above equation is not a function of k.

The array vector associated with a total of U interference signals is given by

$$\underline{x}_u(k) = \sum_{i=1}^{U} \underline{a}_i u_i(k) \tag{3}$$

where $\underline{a}_i$ is the array response to the ith interferer $u_i(k)$. Without loss of generality, we set $\|\underline{h}\|_F^2 = N$ and $\|\underline{a}_i\|_F^2 = N, i = 1, 2, \ldots, U$, where $\|\cdot\|_F$ is the Frobenius norm of a vector. The input data vector is the sum of three components

$$\begin{aligned} \underline{x}(k) &= \underline{x}_s(k) + \underline{x}_u(k) + \underline{b}(k) \\ &= d(k)\underline{h} + \sum_{i=1}^{U} \underline{a}_i u_i(k) + \underline{b}(k) \end{aligned} \tag{4}$$

where $\underline{b}(k)$ is the additive noise vector. With regard to the above equation, we make the following assumptions.

A1)   The information symbols $s(n)$ is a wide-sense stationary process with $E[s(n)s^*(n)] = 1$, where $E[\cdot]$ is the statistical expectation operator, and the superscript * denotes complex conjugation. The spreading sequence $c(k)$ is a binary random sequence with $E[c(k)c(k + l)] = \delta(l)$, where $\delta(l)$ is the delta function.[1]

A2)   The noise vector $\underline{b}(k)$ is zero-mean, temporally and spatially white with

$$E[\underline{b}(k)\underline{b}^T(k + l)] = \mathbf{0} \quad \text{for all } l$$

and

$$E[\underline{b}(k)\underline{b}^H(k + l)] = \sigma\delta(l)\mathbf{I}_N$$

---

[1]This assumption is most suitable for military applications and P-code GPS.
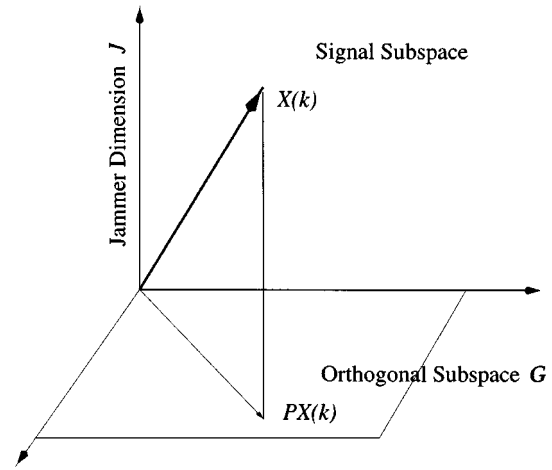

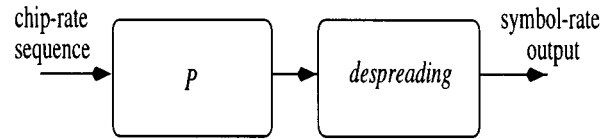Fig. 1.   Jammer suppression by subspace projection.

Fig. 2.   Block diagram of single-sensor subspace projection.

where σ is the noise power, the superscripts T and H denote transpose and conjugate transpose, respectively, and $\mathbf{I}_N$ is the $N \times N$ identity matrix.

A3)   The signal and noise are statistically uncorrelated.

III. SUBSPACE PROJECTION

The aim of subspace projection techniques is to remove the interference components before despreading by projecting the input data on the subspace orthogonal to the interference subspace, as illustrated in Fig. 1. The receiver block diagram is shown in Fig. 2.

A nonstationary interference, such as an FM signal, often shares the same bandwidth with the DS/SS signal and noise. As such, for a chirp signal or a signal with high-order frequency laws, the signal spectrum may span the entire frequency band, and the sample data matrix loses its complex exponential structure responsible for its singularity. Therefore, the interference subspace can no longer be obtained from the eigendecomposition of the sample data matrix [13], [15] or the data covariance matrix [14], as it is typically the case in stationary environments. The nonstationary interference subspace, however, may be constructed using the interference time-frequency signature. Methods for estimating the instantaneous frequency, instantaneous bandwidth, and, more generally, a time–frequency subspace, based on the signal time–frequency localization properties are, respectively, discussed in [15], [18], and [19].

For the general class of FM signals, and providing that interference suppression is performed separately over the different data symbols, the interference subspace is one-dimensional (1-D) in an L-dimensional space. We note that since an FM interference has a constant amplitude, its respective data vector can be determined from the IF up to a complex multiplication factor. The unit norm normalization of this vector represents

the 1-D interference subspace basis vector. Among candidate methods of IF estimation is the one based on the time–frequency distributions. For example, the discrete form of Cohen's class of TFD of a signal $x(t)$ is given by [20]

$$D_{xx}(t,f) = \sum_{m=-\infty}^{\infty} \sum_{\tau=-\infty}^{\infty} \phi(m,\tau)x(t+m+\tau)$$
$$\times x^*(t+m-\tau)e^{-j4\pi f\tau} \quad (5)$$

where $\phi(m,\tau)$ is a time–frequency kernel that could be signal-dependent. The TFD concentrates the interference signal power around the IF and makes it visible in the noise and pseudo-random (PN) sequence background [18], [21]. It has been shown that, for linear FM signals, the Radon–Wigner transform provides improved IF estimates over the TFD [22]. Parametric methods using autoregressive model have also been proposed [23].

Other nonstationary interference with instantaneous bandwidth or spread in the time–frequency domain are captured in a higher dimension subspace. In this case, the interference subspace can be constructed from the interference localization region Ω in the time–frequency domain (see, for example, [15]). The subspace of interest becomes that which fills out the interference time–frequency region Ω energetically but has little or no energy outside Ω.

Interference-free DS/SS signals are obtained by projecting the received data vector (in the temporal domain processing, the vector consists of data samples at different snapshots) on the subspace orthogonal to the interference subspace.

A. Temporal Processing

In the single-sensor receiver, the input data is expressed as

$$x(k) = x_s(k) + x_u(k) + b(k) = d(k) + \sum_{i=1}^{U} u_i(k) + b(k). \quad (6)$$

Using L sequential chip-rate samples of one symbol of the received signals at time index k, we obtain the following input vector:

$$[x(k) \quad x(k-1) \quad \cdots \quad x(k-L+1)]^T$$
$$= [x_s(k) \quad x_s(k-1) \quad \cdots \quad x_s(k-L+1)]^T$$
$$+ [x_u(k) \quad x_u(k-1) \quad \cdots \quad x_u(k-L+1)]^T$$
$$+ [b(k) \quad b(k-1) \quad \cdots \quad b(k-L+1)]^T \quad (7)$$

or simply

$$X(k) = X_s(k) + X_u(k) + B(k). \quad (8)$$

We drop the variable k for simplicity, with the understanding that processing is performed over the nth symbol that starts at the kth chip. Then, (8) becomes

$$X = X_s + X_u + B. \quad (9)$$

Later, we relax the FM condition used in [13], [16] that translates to a single dimension interference. The general case of an interference occupying higher dimension subspace is considered. We assume that the ith interferer spans M_i-dimensional

subspace, which is defined by the orthonormal basis vectors $V_{i,1}, V_{i,2}, \ldots, V_{i,M_i}$, and the different interference subspaces are disjoint. Define

$$V_i = [V_{i,1} \quad V_{i,2} \quad \cdots \quad V_{i,M_i}] \quad (10)$$

and let $M = \sum_{i=1}^{U} M_i$ be the number of total dimensions of the interferers. With $L > M$, the $L \times M$ matrix

$$V = [V_1 \quad V_2 \quad \cdots \quad V_U], \quad V_i \bigcap V_j = \Phi \quad \text{for } i \neq j \quad (11)$$

is full rank, and its columns span the combined interference subspace J. The respective projection matrix is

$$\bar{P} = V(V^H V)^{-1} V^H. \quad (12)$$

The projection matrix associated with the interference orthogonal subspace G is then given by

$$P = \mathbf{I}_L - V(V^H V)^{-1} V^H. \quad (13)$$

When applied to X, matrix P projects the input data vector onto G and results in

$$X_\perp = PX = PX_s + PB \quad (14)$$

which no longer includes any interference component.

The single-sensor receiver implementing subspace projection for excision of a single instantaneously narrowband FM interferer (i.e., $U = 1, M_1 = 1$) in DS/SS communications is derived in [24]. The receiver SINR is shown to be

$$\text{SINR} = \frac{(L-1)^2}{\left(1 - \frac{2}{L}\right) + \sigma(L-1)}$$
$$= \frac{L-1}{\frac{L-2}{L(L-1)} + \sigma}. \quad (15)$$

For typical values of L, $(L-2)/(L-1) \approx 1$, and (15) can be simplified as

$$\text{SINR} \approx \frac{L-1}{\sigma + 1/L}. \quad (16)$$

Compared with the interference-free environment, where the receiver SINR is L/σ, nonstationary interference suppression in (16) is achieved by reducing the processing gain by 1 and increasing the noise power by the self-noise factor of $1/L$.

IV. SUBSPACE PROJECTION IN MULTISENSOR RECEIVER

In this section, we consider nonstationary interference excision in multisensor receivers using subspace projections. We note that if the subspace projection method discussed in Section III is extended to an N-element array by suppressing the interference independently in each sensor data and then combining the results by maximum ratio combining (see Fig. 3), then it is straightforward to show that the receiver SINR is given by

$$\text{SINR} \approx \frac{N(L-1)}{\sigma + N/L}. \quad (17)$$

The above extension, although clearly improved over (16), does not utilize the potential difference in the spatial signatures of
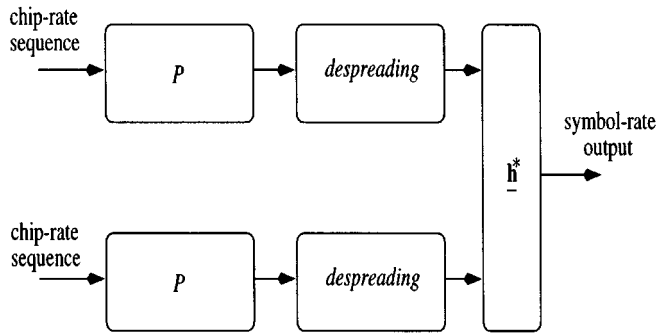
Fig. 3.   Block diagram of independent multisensor subspace projection.

signal arrivals and, therefore, is inferior to the receiver proposed in this section.

A. Spatio-Temporal Signal Subspace Estimation

To construct the spatio-temporal signal subspace of the interference signals, it is important to estimate both the time–frequency signature (or subspace) and the spatial signature of each interferer. The IF estimation of an FM interference signal based on time–frequency distribution is addressed in Section III. It is noteworthy that when multiple antennas are available, the TFD may be computed at each sensor data separately and then averaged over the array. This method has been shown in [25] to improve the IF estimation, as it reduces noise and crossterms that often obscure the source true power localization in the time–frequency domain.

On the other hand, the estimation of source spatial signature can be achieved, for example, by using direction-finding and source-separation techniques. When the interference signals have clear bearings, methods like MUSIC [26] and maximum likelihood (ML) [27] can be used to estimate the steering matrix of the interference signals. These methods can be revised to incorporate the TFD of the signal arrivals for improved performance [28]–[30]. On the other hand, in fading channels where the steering vector loses its known structure due to multipath, blind source separation methods should be used [31]–[33]. Since the interferers in DS/SS communications often have relatively high power, good spatial signature estimation is expected.

More conveniently, the spatial signatures can be simply estimated by using matched filtering once the time–frequency signatures are provided. The maximum likelihood estimator for the vector $\underline{a}_i$ is obtained as

$$\hat{\underline{a}}_i = \sqrt{N} \sum_{k=0}^{L-1} \hat{u}_i^*(k)\underline{x}(k) \Big/ \left\| \sum_{k=0}^{L-1} \hat{u}_i^*(k)\underline{x}(k) \right\|_F \tag{18}$$

where $\hat{u}_i(k)$ is the estimated waveform of the ith interferer. It is noted that the possible phase ambiguity in the waveform estimation of $\hat{u}_i(k)$ does not affect the estimation of the spatial signature. For slowly varying channels, the above average can also be performed over multiple symbols to improve the estimation accuracy.

In the analysis presented herein, we assume knowledge of the interference subspace and its spatial signature to derive the receiver SINR.

B. Proposed Technique

The subspace projection problem for nonstationary interference suppression in DS/SS communications is now considered within the context of multisensor array using N array elements. We use one symbol DS/SS signal duration (i.e., L chip-rate temporal snapshots) and stack L discrete observations to construct an $NL \times 1$ vector of the received signal sequence in the joint spatio-temporal domain. In this case, the received signal vector in (4) becomes

$$\begin{aligned} &[\underline{x}^T(k) \quad \underline{x}^T(k-1) \quad \cdots \quad \underline{x}^T(k-L+1)]^T \\ &= [\underline{x}_s^T(k) \quad \underline{x}_s^T(k-1) \quad \cdots \quad \underline{x}_s^T(k-L+1)]^T \\ &+ [\underline{x}_u^T(k) \quad \underline{x}_u^T(k-1) \quad \cdots \quad \underline{x}_u^T(k-L+1)]^T \\ &+ [\underline{b}^T(k) \quad \underline{b}^T(k-1) \quad \cdots \quad \underline{b}^T(k-L+1)]^T \end{aligned} \tag{19}$$

or simply

$$\mathbf{X} = \mathbf{X}_s + \mathbf{X}_u + \mathbf{B} \tag{20}$$

where again, the variable k is dropped for simplicity.

In (19), the interference vector in the single-sensor problem, which is given by (7), is extended to a higher dimension. With the inclusion of both temporal and spatial samples, the mth basis of the ith interference becomes

$$\mathbf{V}_{i,m} = V_{i,m} \otimes \underline{a}_i \tag{21}$$

and

$$\mathbf{V}_i = [\mathbf{V}_{i,1} \quad \mathbf{V}_{i,2} \quad \cdots \quad \mathbf{V}_{i,M_i}] \tag{22}$$

where $\otimes$ denotes the Kronecker product. The columns of the $LN \times M$ matrix

$$\mathbf{V} = [\mathbf{V}_1 \quad \mathbf{V}_2 \quad \cdots \quad \mathbf{V}_U] \tag{23}$$

spans the overall interference signal subspace.

For independent spatial signatures, the matrix rank is M. The orthogonal projection matrix is given by

$$\mathbf{P} = \mathbf{I}_{LN} - \mathbf{V}(\mathbf{V}^H\mathbf{V})^{-1}\mathbf{V}^H. \tag{24}$$

The projection of the signal vector on the orthogonal subspace of the interferers' yields

$$\mathbf{X}_\perp = \mathbf{P}\mathbf{X} = \mathbf{P}\mathbf{X}_s + \mathbf{P}\mathbf{B}. \tag{25}$$

The block diagram of the proposed method is presented in Fig. 4. As shown in the next section, effective interference suppression can be achieved solely based on the spatial signatures or the time-frequency signatures, or it may require both.

C. Performance Analysis

Later, we consider the performance of the multisensor receiver system implementing subspace projections. Recall that

$$V_{i,m}^H V_{j,n} = 0 \quad \text{for any } i, m \neq j, n. \tag{26}$$

and

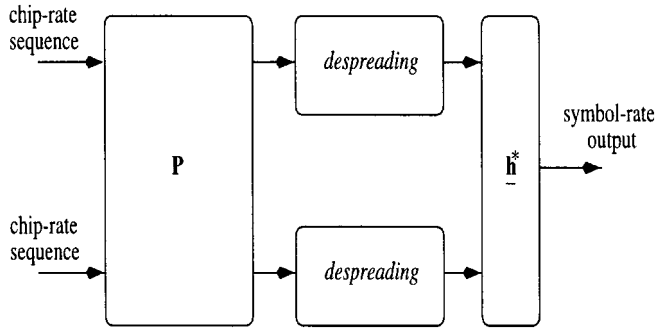$$\mathbf{V}^H\mathbf{V} = N\mathbf{I}_M \tag{27}$$

Fig. 4. Block diagram of proposed multisensor subspace projection.

and the projection matrix $\mathbf{P}$ becomes

$$\mathbf{P} = \mathbf{I}_{LN} - \frac{1}{N} \mathbf{V}\mathbf{V}^H. \tag{28}$$

The signal vector $\mathbf{X}_s$ can be rewritten as

$$
\begin{aligned}
\mathbf{X}_s &= \begin{bmatrix} \underline{x}_s^T(k) & \underline{x}_s^T(k-1) & \cdots & \underline{x}_s^T(k-L+1) \end{bmatrix}^T \\
&= [d(k)\underline{h}^T \quad d(k-1)\underline{h}^T \quad \cdots \quad d(k-L+1)\underline{h}^T]^T \\
&= s(n)[c(L-1) \quad c(L-2) \quad \cdots \quad c(0)]^T \otimes \underline{h} \\
&\triangleq s(n)\mathbf{q}
\end{aligned}
\tag{29}
$$

where the $LN \times 1$ vector

$$
\begin{aligned}
\mathbf{q} &= [c(L-1) \quad c(L-2) \quad \cdots \quad c(0)]^T \otimes \underline{h} \\
&\triangleq \underline{c} \otimes \underline{h}
\end{aligned}
\tag{30}
$$

defines the spatio-temporal signature of the desired DS/SS signal. $\mathbf{q}$ is the extension of the DS/SS code by replicating it with weights defined by the signal spatial signature.

By performing despreading and beamforming, the symbol-rate decision variable is given by

$$
\begin{aligned}
y(n) &= \mathbf{q}^H \mathbf{X}_\perp(k) = s(n)\mathbf{q}^H \mathbf{P}\mathbf{q} + \mathbf{q}^H \mathbf{P}\mathbf{B}(k) \\
&\triangleq y_1(n) + y_2(n)
\end{aligned}
\tag{31}
$$

where $y_1(n)$ is the contribution of the desired DS/SS signal to the decision variable, and $y_2(n)$ is the respective contribution from the noise.

The SINR of the array output becomes (32), shown at the bottom of the page (see also Appendix A), where ξ_i is defined in (A.9), and β_i is the spatial correlation coefficient between the spatial signatures $\underline{h}$ and $\underline{a}_i, i = 1, 2, \ldots, U$ and is given by

$$\beta_i = \frac{1}{N} \underline{h}^H \underline{a}_i. \tag{33}$$

Note that when the noise power is small, i.e., $\sigma \ll 1$, the variance of y_1 becomes dominant, and the output SINR reaches the following upper bound:

$$\text{SINR}_{\text{high SNR}} \approx \frac{\left(L - \sum_{i=1}^{U} M_i |\beta_i|^2\right)^2}{\left(\sum_{i=1}^{U} M_i |\beta_i|^2\right)^2 - 2\sum_{i=1}^{U} \xi_i |\beta_i|^4}. \tag{34}$$

This result is affected by the factors $L, M_i, |\beta_i|$, and $\xi_i, i = 1, \ldots, U$. On the other hand, when the noise level is very high, i.e., $\sigma \gg 1$, the noise variance plays a key role in determining $\text{var}[y(k)]$, and the output SINR becomes

$$
\begin{aligned}
\text{SINR}_{\text{low SNR}} &\approx \frac{\left(L - \sum_{i=1}^{U} M_i |\beta_i|^2\right)^2}{\frac{\sigma}{N}\left(L - \sum_{i=1}^{U} M_i |\beta_i|^2\right)} \\
&= \frac{N}{\sigma}\left(L - \sum_{i=1}^{U} M_i |\beta_i|^2\right).
\end{aligned}
\tag{35}
$$

Unlike the high input SNR case, the output SINR in (35) also depends on both N and σ. Comparing (34) and (35), it is clear that the improvement in the receiver SINR becomes more significant when the spatial signatures produce small spatial correlation coefficients and under high SNR.

Next, we consider some specific important cases. When $\beta_i = 0, i = 1, \ldots, U, \text{var}[y_1(n)] = 0$, the receiver SINR in (32) becomes $\text{SINR} = LN/\sigma$. This is to say, the output SINR is improved by a factor of LN over the input signal-to-noise ratio (SNR) (not the input SINR). This implies that the interferers are suppressed by spatial selectivity of the array, and their suppression does not cause any distortion of the temporal characteristics of the DS/SS signal. The DS/SS signal, in this case, enjoys the array gain that contributes the factor N to the SINR.

For a single FM interferer ($U = 1, M_1 = 1$), (32) becomes

$$\text{SINR} = \frac{(L - |\beta_1|^2)^2}{\left(1 - \frac{2}{L}\right)|\beta_1|^4 + \frac{\sigma}{N}(L - |\beta_1|^2)}. \tag{36}$$

It is easy to show that SINR in (36) monotonously decreases as $|\beta_1|$ increases, and the lower bound of the SINR is reached for $|\beta_1| = 1$, which is the case of the desired DS/SS signal and the interference signal arriving from the same direction. With a unit value of $|\beta_1|$

$$\text{SINR} = \frac{(L-1)^2}{\left(1 - \frac{2}{L}\right) + \frac{\sigma}{N}(L-1)} \approx \frac{N(L-1)}{\sigma + N/L}. \tag{37}$$

This result is the same as that of the single-sensor case developed in [16], except for the appearance of the array gain N for the desired DS/SS signal over the noise. This equation also coincides with (17). That is, the independent multisensor subspace projection illustrated in Fig. 3 results in the same

$$\text{SINR} = \frac{E^2[y(k)]}{\text{var}[y(k)]} = \frac{\left(L - \sum_{i=1}^{U} M_i |\beta_i|^2\right)^2}{\left(\left(\sum_{i=1}^{U} M_i |\beta_i|^2\right)^2 - 2\sum_{i=1}^{U} \xi_i |\beta_i|^4\right) + \frac{\sigma}{N}\left(L - \sum_{i=1}^{U} M_i |\beta_i|^2\right)} \tag{32}$$
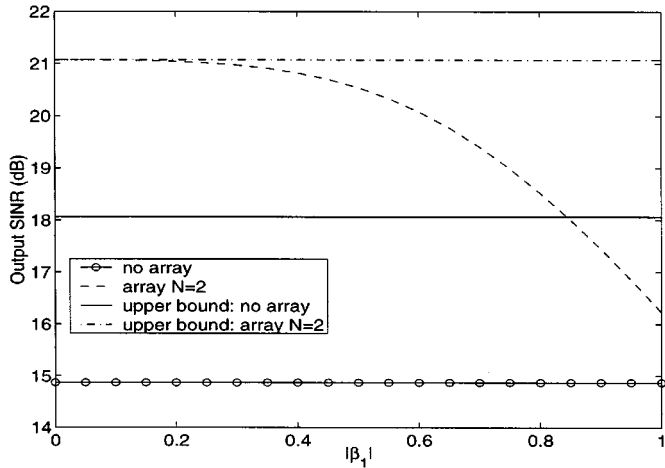
Fig. 5. Output SINR versus $|\beta_1|$ (input SNR = 0 dB, $L = 64, U = 1, M = 7$).

Fig. 6. Output SINR versus input SNR ($L = 64, U = 2, M_1 = M_2 = 7, \theta_D = 0°, \theta_J = [40°, 60°]$).

output SINR with the proposed multisensor subspace projection method when $|\beta_1| = 1$.

On the other hand, the maximum value in (36) corresponds to $\beta = 0$ and is equal to SINR $= LN/\sigma$, as discussed above. For the illustration of the SINR behavior, we plot in Fig. 5 the SINR in (36) versus $|\beta_1|$ for a two-sensor array, where $L = 64$, and one FM jammer is considered with $M = 7$. The input SNR is 0 dB.

Given the temporal and spatial signatures, the proposed technique simplifies to two consecutive tasks. The first is to estimate the spatio-temporal signature. When using multiple antenna receivers, a basis vector of the orthogonal projection matrix is obtained by the Kronecker product of a jammer's temporal signature and its spatial signature, which results in the $LN \times LN$ orthogonal project matrix instead of $L \times L$ in the single antenna case. The second task is jammer suppression via subspace projection. This involves the multiplication of an $LN \times LN$ matrix and an $LN \times 1$ vector.

Note that such an increase in computations is natural due to an increase of dimensionality. It is noteworthy that array processing expands overall space dimensionality but maintains the jammer subspace dimension. As a result, it yields improved SINR performance over temporal processing or spatial processing only methods.

V. NUMERICAL RESULTS

A two-element array is considered with half-wavelength spacing. The DS/SS signal uses random spreading sequence with $L = 64$. The AOA of the DS/SS signal is $0°$ from broadside ($\theta_D = 0°$).

We consider two interference signals. Each interference signal is assumed to be made up of uncorrelated FM component with $M_i = 7, i = 1, 2$. The overall interference subspace is $M = 14$. The AOAs of the two interferers are $\theta_J = [40°, 60°]$. The respective spatial correlations in this example are $|\beta_1| = 0.53$ and $|\beta_2| = 0.21$. Note that in the subspace projection method, the output SINR is independent of the input jammer-to-signal ratio (JSR) since the interferers are entirely suppressed, regardless of their input power. Fig. 6
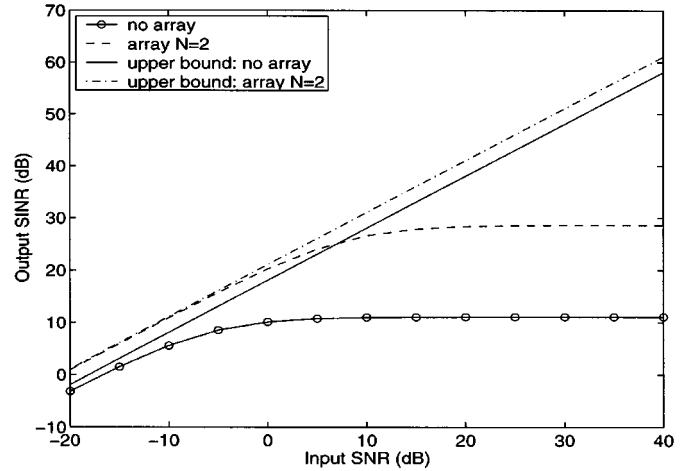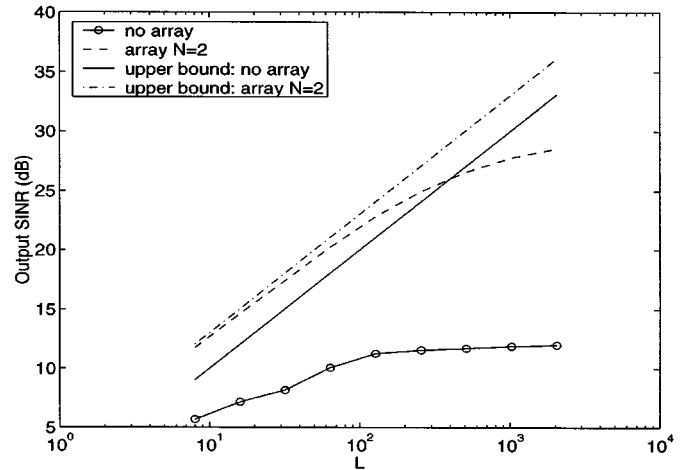

Fig. 7. Output SINR versus the number of chips per symbol (L) (input SNR = 0 dB, $U = 2, M_1 = M_2 = 7, \theta_D = 0°, \theta_J = [40°, 60°]$).

shows the receiver SINR versus the input SNR. The upper bounds correspond to interference-free data. For high input SNR, the receiver SINR is decided by the induced signal distortion described by the variance given in (A.10). It is evident from Fig. 6 that the two-antenna receiver outperforms the single-antenna receiver case by a factor much larger than the array gain. Since the output SINR in the two-antenna receiver highly depends on the spatial correlation coefficients, the curves corresponding to a two-sensor array in Fig. 6 will assume different values upon changing β_1, and/or β_2. The best performance is achieved at $\beta_1 = \beta_2 = 0$.

Fig. 7 shows the receiver SINR versus the number of chips per symbol (L). We let L vary from 8 to 4096, whereas the input SNR is fixed at 0 dB. The two interference signals are incident on the array with angles $\theta_J = [40°, 60°]$. They are assumed to maintain their time–frequency spread with increased value of L. As such, the respective dimensions of their subspaces grow proportionally with the number of chips per symbol. In this example, the dimension of each interference signal is assumed to be 10% of L (round to the nearest integer). The output SINR improvement by performing array processing at different L is evident from this figure. It is seen that unlike the case of the instan-
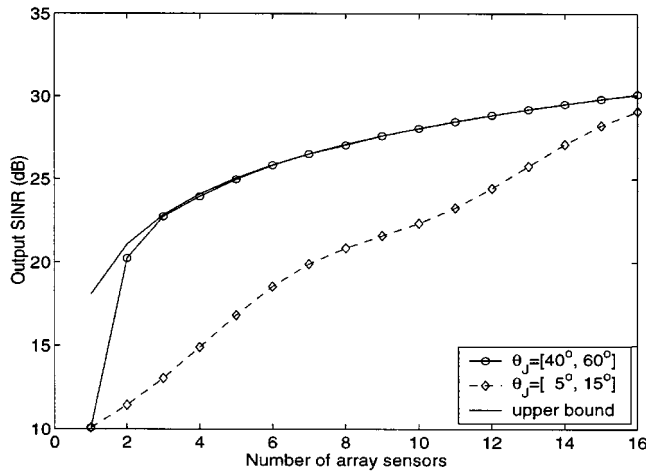
Fig. 8. Output SINR versus the number of array sensors (input SNR $= 0$ dB, $L = 64, U = 2, M_1 = M_2 = 7$).

taneously narrowband FM interference, where the output SINR increases rapidly as L increases, the output SINR in the underlying scenario ceases to increase as L assumes large values. This is because the rank of the interference signal subspace increases with L.

In Fig. 8, we investigate the receiver SINR performance versus the number of array sensors. In this figure, L is set at 64, and the input SNR is 0 dB. Two interference signals composed of uncorrelated FM components are considered, and $M_i = 7, i = 1, 2$ are assumed. Two examples are used to examine the effect of different AOAs. In the first example, $\theta_J = [40°, 60°]$. The output SINR improves sharply as the number of array sensors increases from one to three, beyond which the improvement becomes insignificant. The differences in the above AOAs of the desired DS/SS signal and the interference signals are relatively large, and a small number of array sensors leads to negligible spatial correlation coefficients. We also show a case with closely spaced interference signals where $\theta_J = [5°, 15°]$. In this case, the output SINR slowly improves as the number of array sensors increases.

It is noted that when we consider a specific case, the output SINR does not increase monotonously with the number of array sensors. This is because the relationship between the spatial correlation coefficient and the AOAs is by itself not monotonous. Nevertheless, when we consider the general case with different AOA combinations, a high number of array sensors often reduce the spatial correlation coefficients.

VI. CONCLUSION

In this paper, subspace projection techniques were employed to suppress nonstationary interferers in direct-sequence spread-spectrum (DS/SS) communication systems. Interference suppression is based on the knowledge of both the interference time–frequency and spatial signatures. While the former is based on instantaneous frequency information that can be gained using several methods, including time–frequency distributions, the later can be provided from applying higher resolution methods or blind source separation techniques to the signal arrivals.

The differences between the DS/SS signal and interference signatures both in the time–frequency and spatial domains equip the projection techniques with the ability to remove the interference with a minimum distortion of the desired signal.

The receiver performance based on subspace projections was analyzed. It was shown that the lower performance bound is obtained when the sources have the same angular position. In this case, the problem becomes equivalent to a single-antenna receiver with only the presence of the array gain. On the other hand, the upper bound on performance is reached in the interference-free environment and corresponds to the case in which the spatial signatures of the interference signals are orthogonal to that of the DS/SS signal.

Numerical results were presented to illustrate the receiver SINR dependency on spatial correlation coefficient, input SNR, and the PN sequence length.

APPENDIX A

To derive the output SINR expression, we use $s(n) = +1$ (the output SINR is independent of $s(n)$ and same result follows when $s(n) = -1$). Then

$$
\begin{aligned}
E[y_1(n)] &= E[\mathbf{q}^H \mathbf{P} \mathbf{q}] \\
&= E\left[\mathbf{q}^H \left(\mathbf{I} - \frac{1}{N}\mathbf{V}\mathbf{V}^H\right)\mathbf{q}\right] \\
&= E[\mathbf{q}^H \mathbf{q}] - \frac{1}{N}E[\mathbf{q}^H \mathbf{V}\mathbf{V}^H \mathbf{q}] \\
&= LN - \frac{1}{N}E\left[\mathbf{q}^H \sum_{i_1=1}^{U}\mathbf{V}_{i_1}\sum_{i_2=1}^{U}\mathbf{V}_{i_2}^H \mathbf{q}\right] \\
&= LN - \frac{1}{N}E\left[\mathbf{q}^H \sum_{i_1=1}^{U}\sum_{m_1=1}^{M_i}\mathbf{V}_{i_1,m_1}\right. \\
&\quad \left. \times \sum_{i_2=1}^{U}\sum_{m_2=1}^{M_i}\mathbf{V}_{i_2,m_2}^H \mathbf{q}\right].
\end{aligned} \tag{A.1}
$$

It is straightforward to show that [the definition of β_i is given in (33)]

$$
\begin{aligned}
\mathbf{q}^H \mathbf{V}_{i,m} &= (\underline{c} \otimes \underline{h})^H (V_{i,m} \otimes \underline{a}_i) \\
&= (\underline{c}^T V_{i,m}) \otimes (\underline{h}^H \underline{a}_i) \\
&= N\beta_i \sum_{l=0}^{L-1} V_{i,m}(l)c(l).
\end{aligned} \tag{A.2}
$$

Using the orthogonal property of the spreading sequence A1), (A.1) becomes

$$
\begin{aligned}
E[y_1(n)] &= LN - NE\left[\sum_{i_1=1}^{U}\beta_{i_1}\sum_{m_1=1}^{M_{i_1}}\sum_{l_1=0}^{L-1}V_{i_1,m_1}(l_1)c(l_1)\right. \\
&\quad \left. \times \sum_{i_2=1}^{U}\beta_{i_2}^*\sum_{m_2=1}^{M_{i_2}}\sum_{l_2=0}^{L-1}V_{i_2,m_2}^*(l_2)c(l_2)\right] \\
&= LN - N\sum_{i=1}^{U}|\beta_i|^2\sum_{m=1}^{M_i}\sum_{l=0}^{L-1}|V_{i,m}(l)|^2 c^2(l) \\
&= N\left(L - \sum_{i=1}^{U}M_i|\beta_i|^2\right).
\end{aligned} \tag{A.3}
$$

Due to the zero-mean property of noise (assumption A2), $E[y_2(n)] = 0$. Accordingly

$$E[y(n)] = E[y_1(n)] = N\left(L - \sum_{i=1}^{U} M_i|\beta_i|^2\right). \qquad (A.4)$$

It is clear from (A.4) that the increase in the space dimensionality from L to NL does not simply translate into a corresponding increase in the desired mean value or, subsequently, in the processing gain. In addition, from assumption A3), the cross-correlation between $y_1(n)$ and $y_2(n)$ is zero, i.e.,

$$E[y_1^*(n)y_2(n)] = E[y_1(n)y_2^*(n)] = 0. \qquad (A.5)$$

Therefore, the mean square value of the decision variable is made up of only two terms

$$E[|y(n)|^2] = E[|y_1(n)|^2] + E[|y_2(n)|^2]. \qquad (A.6)$$

The first term is the mean square value of $y_1(n)$. From (26), we have

$$
\begin{aligned}
&E[|y_1(n)|^2]\\
&= E[\mathbf{q}^H \mathbf{P}\mathbf{q}\mathbf{q}^H \mathbf{P}^H \mathbf{q}]\\
&= E\left[\mathbf{q}^H\left(\mathbf{I}_N - \frac{1}{N}\mathbf{V}\mathbf{V}^H\right)\mathbf{q}\mathbf{q}^H\right.\\
&\quad \left.\times \left(\mathbf{I}_{LN} - \frac{1}{LN}\mathbf{V}\mathbf{V}^H\right)\mathbf{q}\right]\\
&= E[\mathbf{q}^H \mathbf{q}\mathbf{q}^H \mathbf{q}] - \frac{2}{N}E[\mathbf{q}^H \mathbf{q}\mathbf{q}^H \mathbf{V}\mathbf{V}^H \mathbf{q}]\\
&\quad + \frac{1}{N^2}E[\mathbf{q}^H \mathbf{V}\mathbf{V}^H \mathbf{q}\mathbf{q}^H \mathbf{V}\mathbf{V}^H \mathbf{q}]\\
&= (LN)^2 - 2LN^2 \sum_{i=1}^{U} M_i|\beta_i|^2\\
&\quad + N^2 E\left[\sum_{i_1=1}^{U} \beta_{i_1} \sum_{m_1=1}^{M_{i_1}} \sum_{l_1=0}^{L-1} V_{i_1,m_1}(l_1)c(l_1)\right.\\
&\quad \times \sum_{i_2=1}^{U} \beta_{i_2}^* \sum_{m_2=1}^{M_{i_2}} \sum_{l_2=0}^{L-1} V_{i_2,m_2}^*(l_2)c(l_2)\\
&\quad \times \sum_{i_3=1}^{U} \beta_{i_3} \sum_{m_3=1}^{M_{i_3}} \sum_{l_3=0}^{L-1} V_{i_3,m_3}(l_3)c(l_3)\\
&\quad \left.\times \sum_{i_4=1}^{U} \beta_{i_4}^* \sum_{m_4=1}^{M_{i_4}} \sum_{l_4=0}^{L-1} V_{i_4,m_4}^*(l_4)c(l_4)\right]\\
&= (LN)^2 - 2LN^2 \sum_{i=1}^{U} M_i|\beta_i|^2\\
&\quad + N^2 E\left[\sum_{i_1=i_2=1}^{U} \beta_{i_1}\beta_{i_2}^* \sum_{m_1=m_2=1}^{M_{i_1}} \sum_{l_1=l_2=0}^{L-1} V_{i_1,m_1}(l_1)\right.\\
&\quad \times V_{i_2,m_2}^*(l_2)c(l_1)c(l_2)\\
&\quad \left.\times \sum_{i_3=i_4=1}^{U} \beta_{i_3}\beta_{i_4}^* \sum_{m_3=m_4=1}^{M_{i_3}} \sum_{l_3=l_4=0}^{L-1} V_{i_3,m_3}(l_3)\right.\\
&\quad \left.\times V_{i_4,m_4}^*(l_4)c(l_3)c(l_4)\right]
\end{aligned}
$$

$$
\begin{aligned}
&+ N^2 E\left[\sum_{i_1=i_4=1}^{U} \beta_{i_1}\beta_{i_4}^* \sum_{m_1=m_4=1}^{M_{i_1}} \sum_{l_1=l_4=0}^{L-1} V_{i_1,m_1}(l_1)\right.\\
&\quad \times V_{i_4,m_4}^*(l_4)c(l_1)c(l_4)\\
&\quad \left.\times \sum_{i_3=i_2=1}^{U} \beta_{i_3}\beta_{i_2}^* \sum_{m_3=m_2=1}^{M_{i_3}} \sum_{l_3=l_2=0}^{L-1} V_{i_3,m_3}(l_3)\right.\\
&\quad \left.\times V_{i_2,m_2}^*(l_2)c(l_3)c(l_2)\right]\\
&+ N^2 E\left[\sum_{i_1=i_3=1}^{U} \beta_{i_1}\beta_{i_3} \sum_{m_1=1}^{M_{i_1}}\sum_{m_3=1}^{M_{i_3}} \sum_{l_1=l_3=0}^{L-1} V_{i_1,m_1}(l_1)\right.\\
&\quad \times V_{i_3,m_3}(l_3)c(l_1)c(l_3)\\
&\quad \times \sum_{i_2=i_4=1}^{U} \beta_{i_2}^*\beta_{i_4}^* \sum_{m_2=1}^{M_{i_2}}\sum_{m_4=1}^{M_{i_4}} \sum_{l_2=l_4=0}^{L-1} V_{i_2,m_2}^*(l_2)\\
&\quad \left.\times V_{i_4,m_4}^*(l_4)c(l_2)c(l_4)\right]\\
&- 2N^2 E\left[\sum_{i_1=i_2=i_3=i_4=1}^{U} \beta_{i_1}\beta_{i_2}^*\beta_{i_3}\beta_{i_4}^*\right.\\
&\quad \times \sum_{m_1=m_2=m_3=m_4=1}^{M_{i_1}} \sum_{l_1=l_2=l_3=l_4=0}^{L-1} V_{i_1,m_1}(l_1)\\
&\quad \left.\times V_{i_2,m_2}^*(l_2)V_{i_3,m_3}(l_3)V_{i_4,m_4}^*(l_4)c(l_1)c(l_2)c(l_3)c(l_4)\right]\\
&= (LN)^2 - 2LN^2 \sum_{i=1}^{U} M_i|\beta_i|^2\\
&\quad + N^2\left(2\left(\sum_{i=1}^{U} M_i|\beta_i|^2\right)^2 + \left|\sum_{i=1}^{U} \beta_i^2\gamma_i\right|^2\right.\\
&\quad \left.- 2\sum_{i=1}^{U} \xi_i|\beta_i|^4\right) \qquad (A.7)
\end{aligned}
$$

where

$$\gamma_i = \sum_{m_1=1}^{M_i}\sum_{m_2=1}^{M_i}\sum_{l=1}^{L-1} V_{i,m_1}(l)V_{i,m_2}(l) \qquad (A.8)$$

and

$$\xi_i = \sum_{m=1}^{M_i}\sum_{l=1}^{L-1} |V_{i,m}(l)|^4. \qquad (A.9)$$

In practice, γ_i takes negligible values, and (A.7) can be simplified to

$$
\begin{aligned}
E[|y_1(n)|^2] &= (LN)^2 - 2LN^2 \sum_{i=1}^{U} M_i|\beta_i|^2\\
&\quad + N^2\left(2\left(\sum_{i=1}^{U} M_i|\beta_i|^2\right)^2 - 2\sum_{i=1}^{U} \xi_i|\beta_i|^4\right). \quad (A.10)
\end{aligned}
$$

The value of ξ_i depends on the type of interference signals. Specifically, when the ith interference signal is made up of a

single FM or a number of uncorrelated FM signal components, then the basis vectors are of constant modulus, and

$$\xi_i = \frac{M_i}{L}. \tag{A.11}$$

The second term of (A.6) is the mean-square value of $y_2(n)$

$$\begin{aligned}
E[|y_2(n)|^2] &= E[\mathbf{q}^H \mathbf{P B}(k) \mathbf{B}^H(k) \mathbf{P}^H \mathbf{q}] \\
&= \sigma E[\mathbf{q}^H \mathbf{P P}^H \mathbf{q}] = \sigma E[\mathbf{q}^H \mathbf{P q}] \\
&= \sigma N \left(L - \sum_{i=1}^{U} M_i |\beta_i|^2 \right).
\end{aligned} \tag{A.12}$$

The variance of $y(n)$ is given by

$$\begin{aligned}
&\text{var}[y(n)] \\
&= E[|y(n)|^2] - E^2[y(n)] \\
&= E[|y_1(n)|^2] + E[|y_2(n)|^2] - E^2[y_1(n)] \\
&= (LN)^2 - 2LN^2 \sum_{i=1}^{U} M_i |\beta_i|^2 \\
&\quad + N^2 \left(2 \left(\sum_{i=1}^{U} M_i |\beta_i|^2 \right)^2 - \frac{1}{L} \sum_{i=1}^{U} M_i |\beta_i|^4 \right) \\
&\quad + \sigma N \left(L - \sum_{i=1}^{U} M_i |\beta_i|^2 \right) - N^2 \left(L - \sum_{i=1}^{U} M_i |\beta_i|^2 \right)^2 \\
&= N^2 \left(\left(\sum_{i=1}^{U} M_i |\beta_i|^2 \right)^2 - 2 \sum_{i=1}^{U} \xi_i |\beta_i|^4 \right) \\
&\quad + \sigma N \left(L - \sum_{i=1}^{U} M_i |\beta_i|^2 \right).
\end{aligned} \tag{A.13}$$

Equation (32) follows by using the results of (A.4) and (A.13).

REFERENCES

[1] H. V. Poor and L. A. Rusch, "Narrowband interference suppression in spread-spectrum CDMA," *IEEE Personal Comm. Mag.*, vol. 1, pp. 14–27, Aug. 1994.

[2] J. D. Laster and J. H. Reed, "Interference rejection in digital wireless communications," *IEEE Signal Processing Mag.*, vol. 14, pp. 37–62, May 1997.

[3] L. B. Milstein, "Interference rejection techniques in spread spectrum communications," *Proc. IEEE*, vol. 76, pp. 657–671, June 1988.

[4] J. Wang and L. B. Milstein, "Adaptive LMS filters for cellular CDMA overlay," *IEEE J. Select. Areas Commun.*, vol. 14, pp. 1548–1559, Oct. 1996.

[5] S. Sandberg, "Adapted demodulation for spread-spectrum receivers which employ transform-domain interference excision," *IEEE Trans. Commun.*, vol. 43, pp. 2502–2510, Sept. 1995.

[6] L. A. Rusch and H. Poor, "Multiuser detection techniques for narrow-band interference suppression in spread spectrum communications," *IEEE Trans. Commun.*, vol. 43, pp. 1725–1737, Feb./Mar./Apr. 1995.

[7] H. Fathallah and L. A. Rusch, "A subspace approach to adaptive narrow-band interference suppression in DSSS," *IEEE Trans. Commun.*, vol. 45, pp. 1575–1585, Dec. 1997.

[8] M. Lops, G. Ricci, and A. T. Tulino, "Narrow-band-interference suppression in multiuser CDMA systems," *IEEE Trans. Signal Processing*, vol. 46, pp. 1163–1175, Sept. 1998.

[9] L. A. Rusch, "MMSE detector for narrow-band interference suppression in DS spread spectrum," in *Proc. Interference Rejection Signal Separation Wireless Commun. Symp.*, Newark, NJ, Mar. 1996.

[10] M. G. Amin and A. Akansu, "Time-frequency for interference excision in spread-spectrum communications," *IEEE Signal Processing Mag.*, vol. 16, Mar. 1999.

[11] M. G. Amin, "Interference mitigation in spread spectrum communication systems using time-frequency distribution," *IEEE Trans. Signal Processing*, vol. 45, pp. 90–102, Jan. 1997.

[12] M. G. Amin, C. Wang, and A. Lindsey, "Optimum interference excision in spread spectrum communications using open loop adaptive filters," *IEEE Trans. Signal Processing*, vol. 47, pp. 1966–1976, July 1999.

[13] B. K. Poh, T. S. Quek, C. M. S. See, and A. C. Kot, "Suppression of strong narrowband interference using eigen-structure-based algorithm," in *Proc. Milcom*, July 1995, pp. 1205–1208.

[14] A. Haimovich and A. Vadhri, "Rejection of narrowband interferences in PN spread spectrum systems using an eigenanalysis approach," *Proc. IEEE Signal Process. Workshop Statist. Signal Array Process.*, pp. 1002–1006, June 1994.

[15] F. Hlawatsch and W. Kozek, "Time-frequency projection filters and time-frequency signal expansions," *IEEE Trans. Signal Processing*, vol. 42, pp. 3321–3334, Dec. 1994.

[16] M. G. Amin and G. R. Mandapati, "Nonstationary interference excision in spread spectrum communications using projection filtering methods," in *Proc. 32nd Annu. Asilomar Conf. Signals, Syst., Comput.*, Pacific Grove, CA, Nov. 1998.

[17] S. Barbarossa and A. Scaglione, "Adaptive time-varying cancellation of wideband interferences in spread-spectrum communications based on time-frequency distributions," *IEEE Trans. Signal Processing*, vol. 47, pp. 957–965, Apr. 1999.

[18] B. Boashash, "Estimating and interpreting the instantaneous frequency of a signal," *Proc. IEEE*, vol. 80, Dec. 1990.

[19] P. Loughlin and K. Davidson, "Instantaneous bandwidth of multicomponent signals," in *Proc. SPIE: Adv. Signal Process. Algorithms, Architectures, Implementations IX*, vol. 3807, July 1999, pp. 546–551.

[20] L. Cohen, *Time-Frequency Analysis*. Englewood Cliffs, NJ: Prentice-Hall, 1995.

[21] P. Rao and F. J. Taylor, "Estimation of the instantaneous frequency using the discrete wigner distribution," *Electron. Lett.*, vol. 26, no. 4, pp. 246–248, Feb. 1990.

[22] M. Wang, A. Chan, and C. Chui, "Linear frequency-modulated signal detection using radon-ambiguity transform," *IEEE Trans. Signal Processing*, vol. 46, pp. 571–586, Mar. 1998.

[23] P. Shan and A. A. Beex, "FM interference suppression in spread spectrum communications using time-varying autoregressive model based instantaneous frequency estimation," *Proc. IEEE Int. Conf. Acoust., Speech, Signal Process.*, pp. 2559–2562, Mar. 1999.

[24] R. S. Ramineni, M. G. Amin, and A. R. Lindsey, "Performance analysis of subspace projection techniques for interference excision in DSSS communications," *Proc. IEEE Int. Conf. Acoust., Speech, Signal Process.*, June 2000.

[25] W. Mu, Y. Zhang, and M. G. Amin, "Bilinear signal synthesis in array processing," *Proc. IEEE Int. Conf. Acoust., Speech, Signal Process.*, May 2001.

[26] R. O. Schmidt, "Multiple emitter location and signal parameter estimation," *IEEE Trans. Antennas Propagat.*, vol. AP-34, pp. 276–280, Mar. 1986.

[27] I. Ziskind and M. Wax, "Maximum likelihood localization of multiple sources by alternating projection," *IEEE Trans. Acoust., Speech, Signal Processing*, vol. 36, pp. 1553–1560, Oct. 1988.

[28] A. Belouchrani and M. Amin, "Time-frequency MUSIC," *IEEE Signal Processing Lett.*, vol. 6, pp. 109–110, May 1999.

[29] Y. Zhang, W. Mu, and M. G. Amin, "Time-frequency maximum likelihood methods for direction finding," *J. Franklin Inst.*, vol. 337, no. 4, pp. 483–497, July 2000.

[30] ——, "Subspace analysis of spatial time-frequency distribution matrices," *IEEE Trans. Signal Processing*, vol. 49, pp. 747–759, Apr. 2001.

[31] J. F. Cardoso, A. Belouchrani, K. A. Maraim, and E. Moulines, "A blind source separation technique using second order statistics," *IEEE Trans. Signal Processing*, vol. 45, pp. 434–444, Feb. 1997.

[32] A. Belouchrani and M. Amin, "Blind source separation based on time-frequency signal representation," *IEEE Trans. Signal Processing*, vol. 46, pp. 2888–2898, Nov. 1998.

[33] Y. Zhang and M. G. Amin, "Blind separation of sources based on their time-frequency signatures," *Proc. IEEE Int. Conf. Acoust., Speech, Signal Process.*, pp. 3132–3135, June 2000.

Yimin Zhang (M'88–SM'01) received the M.S. and Ph.D. degrees from the University of Tsukuba, Tsukuba, Japan, in 1985 and 1988, respectively.

He joined the faculty of the Department of Radio Engineering, Southeast University, Nanjing, China, in 1988. He served as a Technical Manager at Communication Laboratory Japan, Kawasaki, from 1995 to 1997, and as a Visiting Researcher at ATR Adaptive Communications Research Laboratories, Kyoto, Japan, from 1997 to 1998. Currently, he is a Research Fellow with the Department of Electrical and Computer Engineering, Villanova University, Villanova, PA. His current research interests are in the areas of array signal processing, space-time adaptive processing, multiuser detection, blind signal processing, digital mobile communications, and time-frequency analysis.

Moeness G. Amin (F'00) received the B.Sc. degree from Cairo University, Cairo, Egypt, in 1976, the M.Sc. degree from University of Petroleum and Minerals, Dharah, Saudi Arabia, in 1980, and Ph.D. degree in electrical engineering in 1984 from University of Colorado, Boulder.

He has been with the Faculty of the Department of Electrical and Computer Engineering, Villanova University, Villanova, PA, since 1985, where he is now a Professor. His current research interests are in the areas of time–frequency analysis, spread spectrum communications, smart antennas, and blind signal processing.

Dr. Amin was an Associate Editor of IEEE TRANSACTIONS ON SIGNAL PROCESSING from 1995 to 1997 and a member of the Technical Committee of the IEEE Signal Processing Society on Statistical Signal and Array Processing. He is currently a member of the IEEE Signal Processing Society Technical Committee on Signal Processing for Communications. He was the General Chair of the 1994 IEEE International Symposium on Time-Frequency and Time-Scale Analysis and the General Chair of the 2000 IEEE Workshop on Statistical Signal and Array Processing. He received the 1997 IEEE Philadelphia Section Service Award and the IEEE Third Millennium Medal. He also received the 1997 Villanova University Outstanding Faculty Research Award. He serves on the Committee of Science and Arts of the Franklin Institute.